



Non-isothermal devitrification of sodium germanate glasses

M. Catauro*, F. de Gaetano, A. Marotta

Department of Materials and Production Engineering, Piazzale Tecchio, 80125 Napoli, Italy

Received 5 November 2001; received in revised form 10 December 2002; accepted 15 January 2003

Abstract

The devitrification behavior of sodium germanate glasses, examined by Fourier transform infrared spectroscopy, differential thermal analysis and X-ray diffraction is reported. The glass compositions are expressed by the general formula: $x\text{Na}_2\text{O} \cdot (1 - x)\text{GeO}_2$ with $x = 0.100; 0.125; 0.200; 0.250$ and 0.333 . The glass transition temperature values do not change linearly with the increase in Na_2O content but go through a maximum at $x = 0.200$. The phases crystallizing during DTA runs were identified and devitrification mechanisms proposed. The effect on devitrification processes of the specific surface area of the samples was also pointed out.

© 2003 Elsevier Science B.V. All rights reserved.

Keywords: Devitrification; Germanate glasses; Glass transition temperature

1. Introduction

The coordination number of germanium atoms in inorganic glasses has attracted much attention since it is a network forming cation which can be presented in 4-coordinated and 6-coordinated states.

The properties of $\text{R}_2\text{O}-\text{GeO}_2$ glasses have been studied extensively [1–8], especially their density, refractive index and viscosity. These studies indicate that density, refractive index and viscosity pass through a maximum as the R_2O content increases. This behavior was explained [9–12] by the change of the coordination number of Ge atoms from 4 to 6 with the addition of R_2O to GeO_2 glass. Phase equilibria in binary alkali germanate systems have been also reported [5,13].

The present paper is part of a more general study on non isothermal devitrification of germanate glasses. In previous papers [14–17] the effect on devitrification

behavior in germanate glasses of a progressive substitution of Li_2O , K_2O , BaO , and SrO for GeO_2 were reported.

In $\text{Li}_2\text{O}-\text{GeO}_2$ series all glasses studied exhibit internal crystal nucleation without the addition of nucleating agent. The glasses containing 5.0, 12.5, 16.7 and 20 mol% of Li_2O denitrify in more than one step. In the first stage of all glasses metastable $\text{Li}_2\text{Ge}_4\text{O}_9$ microcrystallites are formed initially and are then converted at higher temperatures into the thermodynamic stable phases [14].

In $\text{K}_2\text{O}-\text{GeO}_2$ series the $\text{K}_2\text{O} \cdot 4\text{GeO}_2$ glass exhibit internal crystal nucleation and devitrifies in two steps. Metastable $\text{K}_4\text{Ge}_9\text{O}_{20}$ crystals are initially formed and then converted at higher temperatures into stable $\text{K}_2\text{Ge}_4\text{O}_9$ crystals. $\text{K}_2\text{O} \cdot 7\text{GeO}_2$ and $\text{K}_2\text{O} \cdot 8\text{GeO}_2$ glasses devitrify from the surface into $\text{K}_2\text{Ge}_4\text{O}_9$ crystals [15].

In $\text{BaO}-\text{GeO}_2$ series all the glasses studied show one glass transition temperature except the 5 mol% BaO glass that exhibits two values of glass transition temperature because of a phase separation. In 5, 10,

* Corresponding author. Tel.: +39-081-7682415;

fax: +39-081-7682413.

E-mail address: catauro@unina.it (M. Catauro).

20, 30 mol% BaO glasses only BaGe₄O₉ crystals are formed in the bulk of the samples. The crystallization degree increases with the increase of BaO content. In 40 mol% BaO glass surface crystallization of BaGe₂O₅ and BaGeO₃ occurs [16].

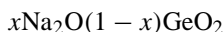
In SrO–GeO₂ series the glasses containing 5.0 and 12.5 mol% of SrO are phase separated. The compositions of the two phases are near to pure vitreous GeO₂ and SrGe₄O₉, respectively. In all the studied glasses the main crystallizing phase is SrGe₄O₉ and grows from bulk nuclei. In powdered samples of glasses containing 5 and 12.5 mol% of SrO the crystallization of GeO₂ also occurs from the surface of glass samples. A small amount of β-SrGeO₃ crystallizes in 25 mol% of SrO [17].

In this work a series of sodium germanate glasses has been studied in order to evaluate the effect of a progressive substitution of Na₂O for GeO₂ on physical properties and devitrification behavior of sodium germanate glasses.

2. Experimental procedures

2.1. Sample preparation

The glass compositions are expressed by the general formula:



with $x = 0.100; 0.125; 0.200; 0.250; 0.333$. In the course of this paper each glass will be named by the corresponding x value. The glasses were prepared by mixing appropriate quantities of ultra pure sodium carbonate and germanium oxide in a batch sized to yield 3 g of glass. The glasses were melted at 1450 °C for 15 min in an uncovered Pt crucible in an electric oven. The crucible containing the glass was weighed both before and after the glass was removed. The weight of the glass agreed with that anticipated from the batch calculation. This result indicates that the actual glass composition is close to that based on the glass batch. The melts were quenched by plunging the bottom of the crucible into cold water. Although this resulted in fracture of the glass, for all the compositions pieces of transparent glass of size sufficient for the experimental measurements were obtained by this technique.

2.2. Characterization

2.2.1. FTIR analysis

Fourier transform infrared (FTIR) absorption spectra were recorded in the 4000–400 cm⁻¹ range using a Mattson 5020 system, equipped with a DTGS KBr (deuterated triglycine sulfate with potassium bromide windows) detector. A spectral resolution of 2 cm⁻¹ was chosen. Each tested sample was mixed with KBr (1 wt.% of the former) in an agate mortar, and then was pressed into 200 mg pellets of 13 mm diameter. The spectrum for each sample represents an average of 20 scans, which were normalized to the spectrum of the blank KBr pellet. The FTIR spectra have been analyzed by Mattson software (FIRST Macros).

2.2.2. DTA analysis

Differential thermal analysis (DTA) curves were recorded in air at a heating rate of 10 °C/min on about 50 mg of bulk or fine powdered (milled in an agate mortar and passed through a 270-mesh sieve) specimens from room temperature to 1000 °C. Powdered Al₂O₃ was added to improve heat transfer between bulk samples and the sample holder. A Netzsch thermoanalyser High Temperature DSC 404 was used with Al₂O₃ as reference material. The experimental error in DTA temperature is ±1 °C. The DTA curves have been elaborated by a Netzsch software.

2.2.3. XRD analysis

The amorphous nature of the glasses and the identification of the phases crystallizing in the glass during the DTA runs were ascertained by X-ray diffraction (XRD) using a Philips diffractometer. Powders of each glass sample were scanned from $2\theta = 5\text{--}60^\circ$ using Cu K α radiation. All the samples were previously heat treated in DTA furnace and then quenched after the DTA run.

3. Results and discussion

The FTIR spectra of the five studied glasses and of GeO₂ glass are shown in Fig. 1. These spectra exhibit broad bands as expected for glassy systems. The highest intensity band at 895 cm⁻¹, due to Ge–O–Ge bond stretching in amorphous GeO₂ shifts (see first column of Table 1) gradually toward a lower wave numbers as

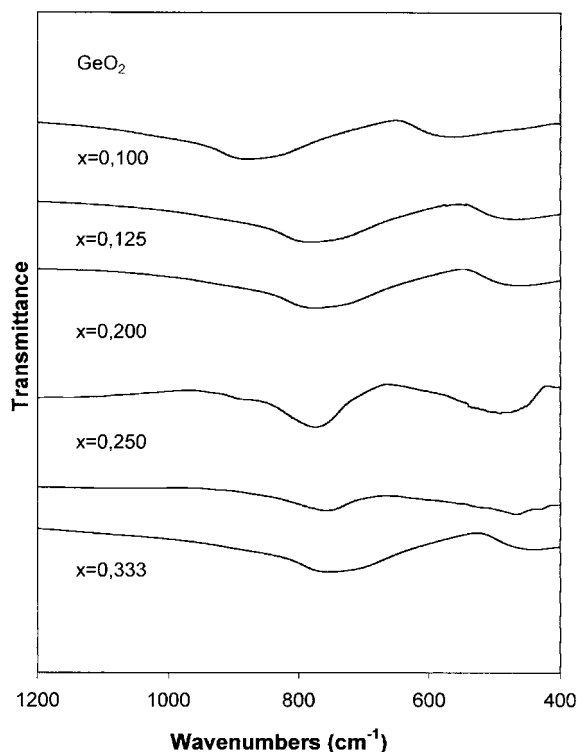


Fig. 1. FTIR transmittance spectra for glasses of composition $x\text{Na}_2\text{O}(1-x)\text{GeO}_2$.

the Na_2O content increases. This shift can be related [9–12] to the change in the coordination number of Ge from 4 to 6. The minus two charge of the GeO_6 octahedra is balanced by the localization of Na^+ ions. The higher the Na_2O content the greater the shift and the $\text{GeO}_6/\text{GeO}_4$ molar ratio. This interpretation is in accordance with the general notion that an increase in co-ordination number from XO_4 to XO_6 causes a decrease in X–O–X stretching frequency [18]. The maximum shift can be observed at about $x = 0.200$.

Table 1

DTA glass transition temperatures T_g and peak temperatures T_p for glasses $x\text{Na}_2\text{O}(1-x)\text{GeO}_2$

Glasses	T_g (°C)	T_p (°C) bulk samples	T_p (°C) powder samples
$x = 0.100$	528	675	638
$x = 0.125$	533	676	640
$x = 0.200$	543	594	594
$x = 0.250$	518	564	564
$x = 0.333$	445	545	516

Fig. 2 shows the DTA curves carried out on bulk samples of the as-quenched glasses. All curves exhibit a slope change followed by an exothermic peak. Glasses with $x = 0.20$ and 0.25 show at higher temperatures a small endo-peak and the glass with $x = 0.33$ shows at higher temperature a great endo-peak.

In this work, the temperature of the inflection point at the slope change of the DTA curve, Fig. 3 was taken as the glass transition temperature, T_g and the values are reported in the first column of Table 1. The T_g values do not change linearly with the increase in Na_2O content but go through a maximum at $x = 0.20$. They clearly show that the glasses investigated exhibit the so-called “germanate anomaly” [1]. This behavior is the result of conversion of germanium ions from four- to six-fold co-ordination with increasing Na_2O content. No non-bridging oxygens are formed. Eventually, however, the formation of six-fold germanium ions reaches a limiting value and non-bridging oxygens begin to form in increasing number. The competitive effects of formation of six-fold coordinated germanium ions and non-bridging oxygens lead to the observed maximum. This hypothesis is supported by the FTIR measurements.

The non isothermal devitrification of glasses is well described by the following equation proposed by Matsumita and Sakka [19]:

$$-\ln(1 - \alpha) = C \left(\frac{N}{\beta^n} \right) \exp \left(-\frac{nE}{RT} \right) \quad (1)$$

where α is the volume fraction crystallized at temperature T , β the DTA heating rate, N the number of nuclei for crystal growth, n a parameter related to the crystallization mechanism, ranging between $n = 1$ for surface nucleation and $n = 3$ for bulk nucleation. The shape of the crystallization peak is related to the parameter n . The higher the value of n , the narrower the peak [20].

The total number of nuclei per unit volume N , is the sum of surface nuclei N_s , bulk nuclei N_h , formed during the DTA run and of bulk nuclei N_n , formed during a previous heat treatment of nucleation [21]. The values of N_s , N_h and N_n are proportional to the specific surface area of the sample, to the reciprocal of the DTA heating rate and the time of the nucleation heat treatment. As in this work the DTA runs were carried out on as-quenched samples $N_n = 0$ and $N = N_s + N_h$. Moreover, it can be easily derived from

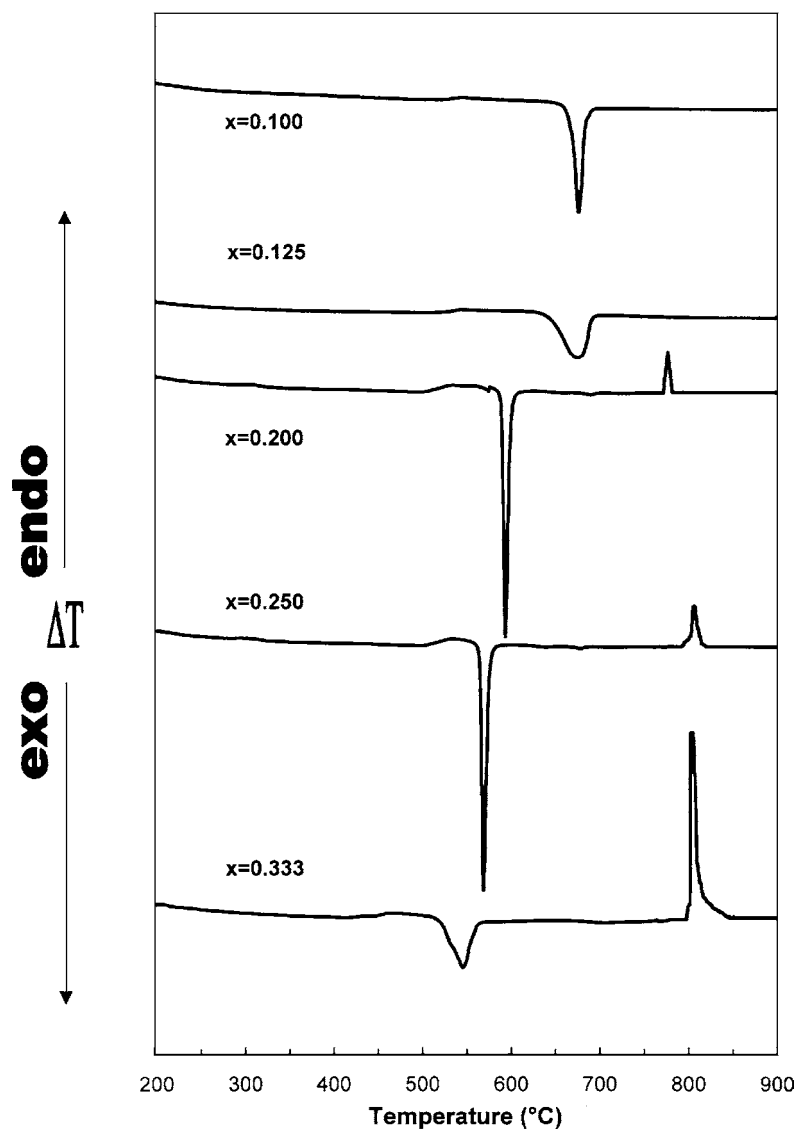


Fig. 2. DTA curves recorded at $10^{\circ}\text{C min}^{-1}$ for glasses of composition $x\text{Na}_2\text{O}(1-x)\text{GeO}_2$.

Eq. (1) that the higher the number of nuclei N , the lower the temperature T_p , of the DTA peak [22].

The shape of the DTA crystallization peaks suggests a bulk crystallization in the glasses with $x = 0.200$ and 0.250 and a surface crystallization in the other glasses. To confirm this hypothesis on the crystallization mechanisms DTA and XRD measurements were therefore carried out on bulk and very fine powdered samples of the investigated glasses.

In Table 1 the temperatures of the crystallization peak detected on DTA curves recorded on powdered samples are compared with those detected on DTA curves recorded on bulk samples. In spite of the great increase of the specific surface area in powdered samples the crystallization peak of glasses with $x = 0.200$ and 0.250 occur at the same temperature (the value of the number of nuclei for unit volume N , is independent by the specific surface area of the samples) and

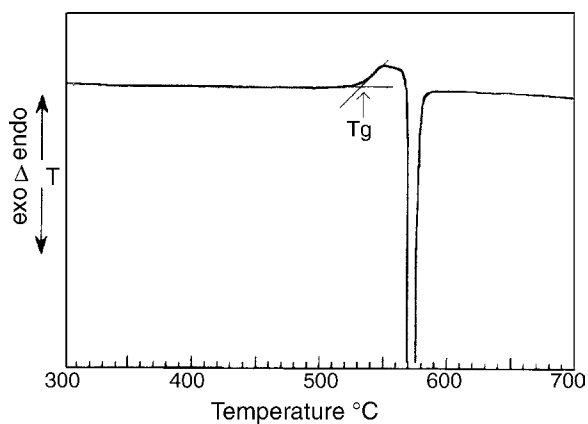


Fig. 3. DTA curve of the term $x = 0.250$ shown on expanded ordinate scale to well display the slope change attributed to the glass transition.

show the same shape on the DTA curves carried out on bulk and powdered samples. These results indicate that in both bulk and powdered samples internal crystallization is dominant $N_h \gg N_s$. Each crystal grow three-dimensionally ($n = 3$) in the bulk of the glass.

On the other hand the DTA curves of glasses $x = 0.100$, 0.125 and 0.333 exhibit broad peaks typical of surface crystallization. Moreover the great increase of specific surface area of powdered samples leads to an increase of surface nuclei so that the DTA crystallization peaks in powdered samples are shifted toward lower temperatures (Table 1). In these glasses surface nucleation is dominant $N_s \gg N_h$. The crystals grow one-dimensionally ($n = 1$) from the surface to the inside of the glass.

In order to identify the phases crystallizing during the DTA runs XRD measurements were carried out on bulk samples heated at $10^\circ\text{C min}^{-1}$ up to temperature of the DTA peak or up to 900°C and then cooled to room temperature.

In the first two terms of the series $x = 0.100$ and 0.125 the XRD patterns of samples heated up to the temperature of the DTA exothermic peak exhibit, Fig. 4, sharp reflections all attributed to $\text{Na}_4\text{Ge}_9\text{O}_{20}$ crystals. On the XRD patterns of samples heated up to 900°C the strongest reflection of GeO_2 crystals was also found.

In the $x = 0.200$ and 0.250 terms of the series the XRD patterns of samples heated up to the temperature of the DTA exothermic peak exhibit several sharp

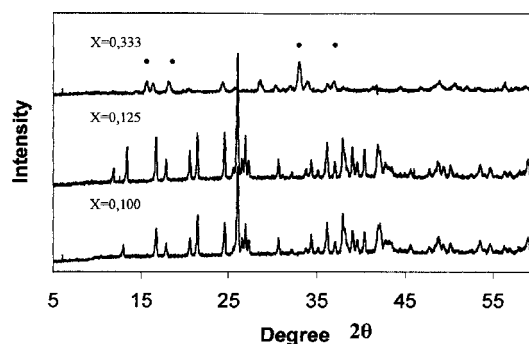


Fig. 4. Powder X-ray diffraction patterns of samples heated up to the DTA exo-peak. Glasses $x = 0.100$ and $x = 0.125$ all lines: $\text{Na}_4\text{Ge}_9\text{O}_{20}$ JCPDS card no. 38-1184. Glass $x = 0.333$ marked lines: Na_2GeO_3 JCPDS card no. 34-693 other lines: $\text{Na}_2\text{Ge}_4\text{O}_9$ JCPDS card no. 21-1352.

lines, Fig. 5b. The major crystalline phase was found to correspond to $\text{Na}_2\text{Ge}_4\text{O}_9$ a phase which is not reported in the $\text{Na}_2\text{O}-\text{GeO}_2$ phase diagram [5] but which has been obtained by reheating a glass of the same composition [23]. In addition to the peaks due to $\text{Na}_2\text{Ge}_4\text{O}_9$ the strongest reflections of $\text{Na}_4\text{Ge}_9\text{O}_{20}$ crystals were also found on these patterns. On the XRD patterns of samples heated up to 900°C , Fig. 5a, all the reflections were attributed to $\text{Na}_4\text{Ge}_9\text{O}_{20}$ crystals. The structure of $\text{Na}_2\text{Ge}_4\text{O}_9$ contains isolated GeO_6 octahedra connected by Ge_3O_9 rings consisting of three GeO_4 tetrahedra to form hexagonal crystals [24]. The oxygen atoms are all of the bridging type; the structure can be described by the formula $\text{Na}_2[\text{Ge}(\text{Ge}_3\text{O}_9)]$. The structure of $\text{Na}_4\text{Ge}_9\text{O}_{20}$ contains chains of GeO_4 tetrahedra connected by Ge_4O_{16} groups which consist of edge shared GeO_6 octahedra to form tetragonal crystals [24]. Thermal phase transitions generally occur from a structure of low symmetry (and high order) to one of higher symmetry (and lower order). In order to get transformation from a low to a high temperature phase the latent heat of transformation, ΔH , must be provided and an endothermic peak appears on the DTA curve. This behavior can be observed in glass with $x = 0.200$ and 0.250 . $\text{Na}_2\text{Ge}_4\text{O}_9$ hexagonal crystals are initially formed and then converted at a higher temperature into $\text{Na}_4\text{Ge}_9\text{O}_{20}$ tetragonal crystals. This transformation from a high order phase to a lower order one involves an endothermic effect on the DTA curve, Fig. 2. If more than one crystal is precipitated from the glass the structure of the metastable phase can

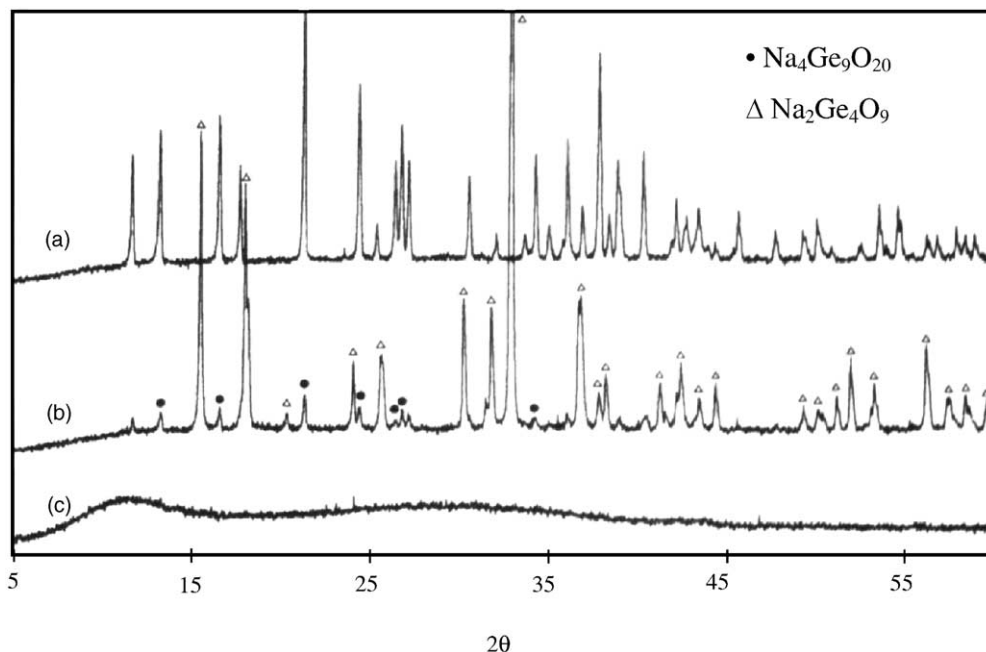


Fig. 5. Powder X-ray diffraction patterns of glass $x = 0.200$: (a) sample after a DTA run up to $900\text{ }^{\circ}\text{C}$; (b) sample up to the DTA exo-peak; (c) as quenched sample.

Table 2
Crystallizing phases during DTA runs

Glasses	$x = 0.100$	$x = 0.125$	$x = 0.200$	$x = 0.250$	$x = 0.333$
Heated up to DTA exo-peak	$\text{Na}_4\text{Ge}_9\text{O}_{20}$	$\text{Na}_4\text{Ge}_9\text{O}_{20}$	$\text{Na}_2\text{Ge}_4\text{O}_9$ $\text{Na}_4\text{Ge}_9\text{O}_{20}(\text{tc})$	$\text{Na}_2\text{Ge}_4\text{O}_9$ $\text{Na}_4\text{Ge}_9\text{O}_{20}(\text{tc})$	$\text{Na}_2\text{Ge}_4\text{O}_9$ Na_2GeO_3
After a DTA run up to $900\text{ }^{\circ}\text{C}$	$\text{Na}_4\text{Ge}_9\text{O}_{20}$ $\text{GeO}_2(\text{tc})$	$\text{Na}_4\text{Ge}_9\text{O}_{20}$ $\text{GeO}_2(\text{tc})$	$\text{Na}_4\text{Ge}_9\text{O}_{20}$	$\text{Na}_4\text{Ge}_9\text{O}_{20}$	Crystals fusion

be supposed to be more like the mother glass than the stable one. In the GeO_6 octahedra may be connected with GeO_4 tetrahedra by sharing corner oxygen and the coalescence of GeO_6 octahedra by sharing edges to Ge_4O_{16} groups may not occur.

Finally in the $x = 0.333$ term of the series the XRD patterns of samples heated up to the temperature of the DTA exothermic peak exhibits, Fig. 4, broad lines. The crystalline phases were found to correspond to Na_2GeO_3 and $\text{Na}_2\text{Ge}_4\text{O}_9$ crystals. The samples heated up to $900\text{ }^{\circ}\text{C}$ were found melted.

The results of the XRD are summarized in Table 2 no appreciable differences between XRD patterns of devitrified bulk and powder samples were found.

4. Conclusions

From the experimental results the following conclusions can be drawn about the non isothermal devitrification of sodium germanate glasses.

- The glass transition temperatures of the investigate glasses do not change linearly with the increase of Na_2O content but go through a maximum at 20 mol% of Na_2O according with the “germanate anomaly”.
- Germanate glasses containing 20 and 25 mol% of Na_2O exhibit internal crystallization without the addition of any nucleating agent. The

devitrification process occurs in both glasses in two steps. Metastable $\text{Na}_2\text{Ge}_4\text{O}_9$ hexagonal crystals are initially formed and then converted at a higher temperature into $\text{Na}_4\text{Ge}_9\text{O}_{20}$ tetragonal crystals.

- (c) In germanate glasses containing 10, 12 and 33 mol% of Na_2O surface crystallization is dominant. The crystallizing phases in 10 and 12 mol% of Na_2O were $\text{Na}_4\text{Ge}_9\text{O}_{20}$ and GeO_2 crystals, in 33 mol% of Na_2O were $\text{Na}_2\text{Ge}_4\text{O}_9$ and Na_2GeO_3 crystals.

References

- [1] K.S. Evstropiev, A.O. Ivanov, *Advances in Glass Technology*, in: F.R. Matson, G.E. Rindone (Eds.), Plenum Press, New York, 1963, Part 2, p. 79.
- [2] M.K. Murthy, J. Ip, *Nature (London)* 201 (1964) 3285.
- [3] J.E. Shelby, *J. Am. Ceram. Soc.* 57 (1974) 436.
- [4] S.V. Nemilov, *J. Appl. Chem. USSR* 43 (1970) 2644.
- [5] M.K. Murthy, J. Aguayo, *J. Am. Ceram. Soc.* 47 (1964) 444.
- [6] M.N. Khan, E.E. Khawaja, *Phys. Status Solidi* 74 (1982) 273.
- [7] K. Takahashi, T. Yoshio, K. Maruoka, *J. Ceram. Ass. Jpn.* 82 (1974) 193.
- [8] K. Takahashi, T. Yoshio, *J. Ceram. Ass. Jpn.* 26 (1977) 785.
- [9] M.K. Murthy, E.M. Kirby, *Phys. Chem. Glasses* 5 (1964) 144.
- [10] S. Sakka, K. Kamiya, *J. Non-Cryst. Solids* 49 (1982) 103.
- [11] H. Verweij, J.H.J.M. Buster, *J. Non-Cryst. Solids* 34 (1979) 81.
- [12] T. Furukawa, W.B. White, *J. Mater. Sci.* 15 (1980) 1648.
- [13] E.M. Levin, C.R. Robins, H.C. McMurdie, *Phase Diagrams for Ceramists*, American Ceramic Society, Columbus, OH, 1964, p. 93.
- [14] A. Marotta, P. Pernice, A. Aronne, M. Catauro, *J. Thermal Anal.* 40 (1993) 181.
- [15] G. Laudisio, M. Catauro, *J. Thermal Anal.* 52 (1998) 967.
- [16] P. Pernice, A. Aronne, M. Catauro, A. Marotta *Phys. Chem. Glasses* 37 (1996) 134.
- [17] G. Laudisio, M. Catauro, G. Luciani, *Phys. Chem. Glasses* 38 (1997) 244.
- [18] J. Wong, C.A. Angell, *Glass Structure by Spectroscopy*, Marcel Dekker, New York, 1976, p. 456.
- [19] K. Matusita, S. Sakka, *Chem. Bull. Inst. Res. Kyoto Univ.* 59 (1981) 159.
- [20] J. Burke, *Le cinétique des Changement de Phase dans les Metaux*, Masson, Paris, 1968, p. 209.
- [21] W.W. Wendlandt, *Thermal Analysis*, Wiley, New York, 1986, p. 448.
- [22] A. Marotta, A. Buri, F. Branda, *J. Mater. Sci.* 16 (1981) 341.
- [23] A. Wittmann, P. Papamantellos, *Mh. Chem.* 92 (1960) 855.
- [24] K. Kamiya, T. Yoko, Y. Itoh, S. Sakka, *J. Non-Cryst. Solids* 91 (1987) 279.